④

MORPHOLOGY OF HIGHLY TEXTURED HDPE

H.H. Song, A.S. Argon and R.E. Cohen
Massachusetts Institute of Technology
Cambridge, MA 02139

Abstract

High density polyethylene (HDPE) specimens were subjected to high orientation producing deformations below the melting point using either a rolling mill or a channel-die. After appropriate annealing protocols, the crystallographic and morphological textures were examined using wide-angle x-ray diffraction pole figures, two-dimensional small-angle x-ray scattering and transmission electron microscopy. Although the two deformation patterns resulted in very similar crystallographic textures, the details of the morphological arrangements of crystalline lamellae were different. Quantitative considerations of the 2-D SAXS patterns led to the conclusion that lamellae which are inclined to the macroscopic orientation direction reflect a shear process within the individual lamellae, rather than a rigid rotation inside the surrounding amorphous material.

89 6 13 153

REPORT DOCUMENTATION PAGE

1a REPORT SECURITY CLASSIFICATION UNCLASSIFIED			1b RESTRICTIVE MARKINGS NONE			
2a SECURITY CLASSIFICATION AUTHORITY			3 DISTRIBUTION/AVAILABILITY OF REPORT Approved for public release. Distribution unlimited.			
2b DECLASSIFICATION/DOWNGRADING SCHEDULE						
4 PERFORMING ORGANIZATION REPORT NUMBER(S) Technical Report No. 18			5 MONITORING ORGANIZATION REPORT NUMBER(S)			
6a NAME OF PERFORMING ORGANIZATION Massachusetts Institute of Technology		6b OFFICE SYMBOL (If applicable)	7a NAME OF MONITORING ORGANIZATION ONR			
6c ADDRESS (City, State, and ZIP Code) 77 Massachusetts Avenue, Room 1-306 Cambridge, MA 02139			7b ADDRESS (City, State, and ZIP Code) 800 North Quincy Street Arlington, VA 22217			
8a NAME OF FUNDING/SPONSORING ORGANIZATION DARPA		8b OFFICE SYMBOL (If applicable)	9 PROCUREMENT INSTRUMENT IDENTIFICATION NUMBER N00014-86-K-0768			
8c ADDRESS (City, State, and ZIP Code) 1400 Wilson Boulevard Arlington, VA 22209			10 SOURCE OF FUNDING NUMBERS			
			PROGRAM ELEMENT NO. R & T Code	PROJECT NO. A 400005	TASK NO	WORK UNIT ACCESSION NO.

11 TITLE (Include Security Classification)
SIMULATION OF TEXTURE EVOLUTION IN DEFORMED SEMI-CRYSTALLINE POLYMERS

12. PERSONAL AUTHOR(S)
Said Ahzi, David M. Parks, and Ali S. Argon

13a TYPE OF REPORT Abstract	13b TIME COVERED FROM 1988 TO 1989	14 DATE OF REPORT (Year, Month, Day) 1989 May 29	15 PAGE COUNT 1

16. SUPPLEMENTARY NOTATION
Abstract of oral presentation to be made at the ASM Symposium on Textures in Non-Metallic Materials on October 2-3, 1989 at Indianapolis, Indiana.

17	COSATI CODES		18 SUBJECT TERMS (Continue on reverse if necessary and identify by block number)
FIELD	GROUP	SUB-GROUP	Simulation of large strain plastic flow in semi-
			crystalline polymers, polyethylene, texture evolution.

19 ABSTRACT (Continue on reverse if necessary and identify by block number)

As in metals, the semi-crystalline polymers can be highly textured by forming (rolling, drawing,...). The crystalline part can deform by slip, twinning or stress-induced martensitic transformation. The goal is to simulate the texture evolution at large deformations and compare results to the experimental ones. The simulation is done by a Relaxed Hybrid model which accounts for the inextensibility of lamellae in the chain direction and by a Self-Consistent model. The amorphous behavior is included in a composite formulation of both models. Results of simulation are in good agreement with experiments in the literature, and also with those obtained in an associated experimental program (H. Song, R. Cohen, and A. Argon).

20 DISTRIBUTION/AVAILABILITY OF ABSTRACT ☒ UNCLASSIFIED/UNLIMITED ☐ SAME AS RPT ☐ DTIC USERS	21 ABSTRACT SECURITY CLASSIFICATION Unclassified	
22a NAME OF RESPONSIBLE INDIVIDUAL Dr. Kenneth Wynne	22b TELEPHONE (Include Area Code) (202) 696-4410	22c OFFICE SYMBOL

1.   Introduction

Modification of semicrystalline polymers from a spherulitic structure to a single crystal-like structure can be effectively achieved by rolling [1] or by channel-die compression [2]. The microstructural arrangements of such oriented semicrystalline polymers are characterized by determining the orientation of crystallographic planes and by the morphology of lamellar stacks. The spatial distribution of the crystallographic planes (pole density) can be precisely measured by wide angle x-ray diffraction (WAXD). The lamellar structure and its orientation, on the other hand, can be analyzed by 2-D small angle x-ray scattering (SAXS). Although 2-D SAXS has been used extensively in the past to reveal the lamellar morphology, or so-called long period of oriented polymers, the interpretation of the 2-D SAXS patterns has been controversial [3-5].

The difficulties in interpretation are partially due to the fact that there is no unique lamellar structure, especially in an oriented polymer, but also due to the inherent characteristics of the scattering method itself (since it is impossible to determine the electron density function $\rho(r)$ of scattering matter directly from the x-ray data). To overcome this problem, transmission electron microscopy (TEM) can be used as a complementary method to SAXS. TEM has proven to be very effective in revealing the local lamellar structure, especially of polyethylene (PE) for which an effective staining technique had been developed by Kanig [6] to delineate the interlamellar amorphous regions. Several TEM studies utilizing this staining technique to reveal the lamellar structure of rolled PE have been published [7,8]. There have been no corresponding studies of the lamellar structure of polymers oriented by channel-die compression, which can give more perfect, quasi-single crystalline textures in relatively bulky specimens; this large specimen size makes the channel-die a useful tool in the investigation of the anisotropic plastic behavior of crystallizable polymers.

The principal aim of this investigation was to reveal the lamellar morphology of HDPE oriented by channel-die compression, and to compare it with the morphology of HDPE obtained by rolling. A secondary aim was to find a general interpretation of the peculiar 2-D SAXS patterns exhibited by these specimens, using TEM micrographs for guidance.

2. Experimental Details

2.1 Materials and Sample Preparation

The material used in this study was high density polyethylene supplied by the USI chemical company. Its molecular weight was $M_w = 55,000$, with a poly-dispersity ratio M_w/M_n of 4.8. The degree of crystallinity based on density measurements was 74%. The polymer pellets were compression molded into certain shapes using a hydraulic press to obtain suitable samples for subsequent orientation. The final orientation of these samples was achieved by channel-die compression and by rolling. In both cases the specimens were oriented at a temperature of 100°C. The thickness reduction in both cases was $\lambda = 6$ (from 3mm to 0.5mm by rolling and from 6cm to 1cm by channel-die compression). The oriented specimens were subsequently annealed in an unconstrained state for 7 hours at 117°C before characterizing their structures. The oriented and annealed samples had degrees of crystallinity in the range of 80% based on density measurements.

2.2 Transmission Electron Microscopy

Transmission electron micrographs were obtained on a Phillips 300 electron microscope operated at 100kV. The specimens were stained [9] with chlorosulfonic acid, without using uranyl acetate to enhance the contrast between the amorphous and crystalline layers. After staining, the specimens became dark and very brittle, indicating that the rubbery amorphous part becomes extensively cross linked in the staining process by the acid. The samples were then microtomed in a LKB ultramicrotome fitted with freshly prepared glass knives.

2.3 X-Ray Measurement

The overall orientations of crystallographic planes of the oriented samples were determined by means of an automated computer-controlled Rigaku WAXD system consisting of a pole figure device associated with a wide angle goniometer coupled to a (Cu radiation) rotating anode x-ray generator operating at 50kV and 60mA. The 2-D SAXS measurements were performed with assistance of a separate

automated computer-controlled system consisting of a Nicolet 2-D position sensitive detector and a Rigaku rotating anode (40kV and 30mA) x-ray generator. The primary beam was collimated by a special two mirror collimator [10]. In this way the x-ray beam could be effectively focused onto a beam-stop with a very fine size without losing much intensity. The specimen to detector distance of the SAXS system was 135cm; the scattered beam path-way between specimen and detector was filled with He gas to minimize attenuation and background scattering.

3. Results and Discussion

3.1 Transmission Electron Microscopy

The superimposed pole figures of the crystallographic planes (200) (020) (002) of a typical HDPE specimen after rolling or channel-die compression followed by annealing is shown in Fig. 1a. The results show that the crystallographic axes a,b,c can be uniquely defined against the macroscopic specimen axes as is shown in Fig. 1b.

Specimens were stained and microtomed, as described above, such that the thin section is parallel to either the (200) plane or the (020) plane. The micrographs thus obtained by TEM are shown in Figs. 2a-b and 3a-b. Figures 2a-b and 3a-b are micrographs of a channel-die compressed sample and a rolled sample, respectively. Here Fig. 2b and Fig. 3b are the micrographs of specimens microtomed parallel to the (200) plane and Figs. 2a and 3a are from sections microtomed parallel to the (020) plane. Oriented lamellar stacks are clearly visible in all the micrographs in which black regions represent the stained interlamellar amorphous material. The unusually thick black features suggest either overstaining or swelling of the amorphous layers. Comparing the micrographs of rolled samples with those obtained from channel-die compression, one main feature is apparent. The micrographs of the channel-die sample in Figs. 2a-b, show remarkably well ordered lamellar stacks with very large dimensions in both a and b directions, while the rolled sample, shown in Figs. 3a-b, shows a corrugated state with relatively smaller lamellar widths of about 1000Å. Both the rolled and channel-die compression samples, however, show similar features in the lamellar orientation and a comparable interlamellar spacing of about 300Å. As shown in the micrographs of Fig. 2a and Fig. 3a, viewed from a direction

parallel to the b-axis, the lamellar surface normals are tilted with respect to the chain c-axis; viewing parallel to the a-axis, the long directions of the lamellae are stacked parallel to the b-axis (Figs. 2b and 3b). Such lamellar orientation suggests that the lamellae are stacked in a sheared state with respect to the flow direction (c-axis direction) mainly on the (200) crystallographic plane.

3.2 2-D Small Angle X-ray Scattering

The same specimens were also studied by 2-D SAXS. The patterns obtained from the channel-die specimen are shown in Figs. 4a-d. Here Fig. 4a was obtained with the x-ray beam parallel to the b-axis. Figures 4b-d view the specimen generally in the direction of the a-axis but are obtained with the specimen rotated around the b-axis so that the x-ray beam is: parallel to the a-axis (Fig. 4b); inclined at 20° with respect to the a-axis (Fig. 4c); and at a 40° inclination with respect to the a-axis (Fig. 4d). Comparison of Fig. 4a and Fig. 4b shows important differences in the SAXS patterns depending on the direction of viewing the specimen; these differences effectively complement the TEM observations presented above.

The diffraction pattern of Fig. 4a, obtained with the x-ray beam parallel to the b-axis, shows unusually spread out diffraction maxima in the equatorial direction, while the Figs. 4b-d show typical compact point patterns. The interpretation of the origin of such broad small angle maxima in the equatorial direction has been controversial, since Hess and Kiessig [11] first reported such patterns for hot-stretched polymers. We will discuss a new model for such elongated patterns in the next section. We note here that Figs. 4b-d show clearly that the scattering maxima shift to higher angles with increase in the angle of tilt away from the a-axis; this means that the lamellar stacks of large tilt with respect to the a-axis possess smaller spacings. The long-spacing obtained from Figs. 4a and 4b is 280Å.

The SAXS patterns from a rolled sample, measured in a similar manner, are shown in Figs. 5a-n. Since it is well known [1] that in a rolled sample the lamellar orientation varies along the sample cross section, the intensities were measured at the center and at the edge of the sample cross section. Here Figs.

5a and 5b represent the patterns viewing the samples parallel to the b-axis: where in Fig. 5a, the beam is at the center, and is covering the whole cross section of rolled sample, and in Fig. 5b the beam is viewing the edge of the cross section. The results show the double lamellar texture with respect to the center line of the cross section as expected [1]. The pattern in Fig. 5a, at first glance, appears to be a typical 4-point pattern, as often observed by other workers [1,12]. In fact, the dumbbell-like pattern also contains two equatorially spread maxima similar to the one observed in the channel-die sample of Fig. 4a, but with broader edges in the vertical direction. The patterns obtained with the beam making angles of 0°, 20°, and 40° with respect to the a-axis of the rolled specimen are shown in Figs. 5c-e. It is interesting to note that the SAXS patterns become broader in the vertical direction as well as shifting to the larger angles as the rotation angle with respect to the a-axis increases. No such broadening effect is observed in the channel die sample of Figs. 5b-5e. These results imply that the broad edge in a dumbbell-shaped pattern of Fig. 5a, and the vertically spread out patterns of Figs. 5d-e are arising from the same lamellar units, as will be discussed further in the next section.

4.   Interpretation of the SAXS Patterns

The x-ray diffraction intensity $I(q)$ from a crystal is given by

$$I(q) = |A(q)|^2 \cdot Z(q) * |S(q)|^2. \tag{1}$$

Here q is the reciprocal lattice vector and * denotes the convolution product. Applying Eq. (1) to a crystal structure of lamellar stacks, $A(q)$ then represents the structure factor of a single lamellar unit and forms a central scattering pattern at very small angles. $Z(q)$ is the reciprocal lattice function that defines the lamellar periodicity and thus the position of diffraction. $S(q)$ is the form factor, which describes the exterior shape of the lamellar stacks. $A(q)$ and $S(q)$ are determined by the sizes of the scattering units, i.e., single lamellar units for $A(q)$ or bundles of lamellae $S(q)$. These two functions can contribute to broadening of the maxima in either the equatorial or the meridional

direction, assuming an ideal lattice function Z(q). For example, maxima are narrow in the meridional direction for large lamellar stacks, and the breadth increases when the size of the stack decreases. Generally, S(q) is a much narrower function than A(q) and therefore the lateral widths of the individual lamellae have been assumed to play the predominant role in equatorial broadening of maxima; this lateral size effect was initially applied by Hess and Kiessig [11] and later by others [12-14] in an attempt to explain the equatorial spread of maxima obtained from oriented semicrystalline polymers. This naturally led to an interpretation that the spread out diffraction spots were due to narrow microfibrils of approximately 100Å width; the lateral dimensions of such microfibrils can be calculated via Guinier plots [15] of the horizontal intensity profiles of the maxima. Recalling our TEM and SAXS patterns presented above, the conventional interpretation for the horizontal spread of the SAXS spots fails immediately; the lamellar widths seen in TEM are far too large to give such broad maxima in the equatorial direction based on the lamellar width alone (Figs. 4a and 5a). Also, the lateral breadths of the SAXS maxima are very different depending on the viewing direction, although the TEM micrographs show comparable lamellar sizes viewed in both a and b directions. Another interpretation was given by Bonart [16] who attributed such broadening effects to a paracrystalline layer lattice model [17] with fluctuations of lattice points, Z(q), in the horizontal direction. Applying Bonart's ideas to our data in Figs. 4a and 5a, we would have to conclude that the lamellae must be stacked in the meridional direction and that the lamellar surfaces are parallel to the equatorial direction with some degree of fluctuation which determines the lateral breadth of the maxima. However the micrographs of Figs. 2a-b and Figs. 3a-b reveal entirely different lamellar orientation; the lamellar surface normals are rather tilted with respect to the c-axis.

We interpret the broad maxima in the horizontal direction, observed in both the channel-die and rolled sample, as simply a composite of diffraction patterns arising from lamellar stacks sheared at different levels, thus having different lamellar surface angles. The schematics shown in Figs. 6a-b describe the lamellar stacks with different levels of shear and the corresponding 2-D SAXS pattern expected from these stacks; note that the thickness, $Dcos\theta$, of the individual lamellar crystallite (as measured by the perpendicular distance

between its surfaces) decreases as the angle of shear θ increases if we take the distance D to be fixed. This restriction of D is reasonable since it represents a constant HDPE crystalline stem-length in the flow direction (Recall that the molecular chain c-axis and the orientation direction are always parallel, (Figs. 1a-b), for both channel-die compressed and rolled specimens regardless of the morphological features, including tilted lamellae, seen in the specimens). A constant molecular stem-length in the c-direction in the crystalline lamellae could reflect either a chain-slip shear process in preformed chain-folded lamellae whose faces were originally perpendicular to the flow direction or it could represent a meandering crystallization process in which highly oriented chains crystallize into lamellar stacks in the presence of the stress fields associated with the imposed deformation process. That the observed SAXS patterns are not a result of rigid rotations of lamellar stacks, in which the lamellar thickness perpendicular to the faces remains constant, is eminently clear from Fig. 7. Here the shear-free rigid rotation of stacks produces a curved SAXS pattern representing a section of the circular pattern expected from randomly distributed identical stacks, i.e., a powder pattern. Thus we conclude that the SAXS pattern shown in Fig. 6c is a superposition of individual patterns of lamellar stacks with different amounts of shear. Recently Blöch and Owen [8], based on the results of electron micrographs, have applied the same idea to simulate the lateral breadth of 4-point patterns, which showed good agreement with the small angle x-ray results.

Since the observed small angle diffraction intensity arises only from those particular lamellae which are aligned parallel to the x-ray beam, it is clear that the intensities and spacings should vary as our specimens are rotated around the b-axis. Experiments were conducted so that the beam entered the specimen at different angles θ (0°-50°) to the a-axis, to observe the contributions of those lamellar stacks tilted with the same angle θ to the c-axis. Some of the results ($\theta = 0°$, 20°, 40°) were shown in the Figs. 4b-d (channel-die compression) and in the Figs. 5c-e (rolling). If the constant-stem-length sheared-lamellae model proposed here is correct, the observed spacings from these experiments D_θ should depend on the rotation angle θ as follows:

$$D_\theta = D\cos\theta, \qquad (2)$$

where D is the invariant stem-length; D is also the thickness of those lamellae whose normals are exactly parallel ($\theta = 0$) to the c-axis or flow direction. Figure 8 is a plot of the normalized long period, D/D_{θ}, obtained from these rotation experiments on both the channel-die compressed and rolled specimens, as a function of the rotation angle θ. The agreement with the function $\cos\theta$, as anticipated from Eq. (2), is quite good lending support to the overall interpretations given here.

Finally, some information on the relative populations of lamellar stacks at various angles can be obtained by the equatorial intensity profile of the SAXS maxima. Figure 9 is a plot of normalized intensity profile (relative to I at the center of the maxima) as a function of tilt angle θ for the two types of specimen studied here. The tilt angle θ in the figure is derived from $\cos^{-1}(D_{\theta}/D)$. Interestingly, the morphological texture, as reflected in the relative amounts of lamellae in each orientation in the material, is quite different for the rolled material and the channel-die compressed specimen. In the former there is some preference for lamellae to lie inclined at 20-30° to the chain c-axis, whereas in the channel-die compressed material the relative population of lamellae drops monotonically with angle.

5.   Conclusions

Electron micrographs have revealed that two samples of HDPE which were oriented by channel-die compression and by rol'ing possess distinctly different lamellar morphologies, even though the two samples are very similar in regard to crystallographic orientation relative to macroscopic specimen axes. The channel-die sample showed well ordered lamellar stacks of large dimensions, but the rolled sample showed a corrugated state. Combining the results of micrographs and 2-D SAXS, we conclude that the lamellae in both samples are stacked in a sheared state toward the c-axis, so the lamellar surface normals are tilted in the a-c plane. Broad SAXS maxima in the equatorial direction, observed with the beam parallel to the b-axis, were then interpreted as a superposition of individual patterns of lamellar stacks sheared at different levels, thus having different surface angles and different lamellar thicknesses.

6. Acknowledgements

References

1. Pope, D.P.; Keller, A.; J. Materials Sci. 9 (1974) 920.

2. Gray, R.W.; Young, R.J.; J. Materials Sci. 9 (Letters) (1974) 521.

3. Cowking, A.; Rider, J.G.; Hay, I.L.; Keller, A.; J. Materials Sci. 3 (1968) 646.

4. Groves, G.W.; Hirsch, P.B.; J. Materials Sci. 4 (Letters) (1969) 929.

5. Hosemann, R.; Loboda-Cackovic, J.; Kaji, K.: J. Appl. Cryst. 11 (1978) 540.

6. Kanig, G.; Kolloid Z.u.Z. Polymere 251 (1973) 782.

7. Grubb, D.T.; Dlugosz, J.; Keller, A.; J. Materials Sci. 10 (Letters) (1975) 1826.

8. Blöch, C.; Owen, A.J.; Coll. Polym. Sci. 262 (1984) 793.

9. Hodge, A.M.; Basset, D.C.; J. Materials Sci. 12 (1977) 2065.

10. Franks, A.; Proc. Phys. Soc. (London) B68 (1955) 1054.

11. Hess, K.; Kiessig, H.; Z. Physik. Chem. A193 (1944) 196.

12. Belbeoch, B.; Guinier, A.; Makromol. Chem. 31 (1951) 1.

13. Bonart, R.: Hosemann, R.; Kolloid Z.Z. Polym. 186 (1962) 16.

14. Statton, W.O.; Goddard, G.M.; J. Appl. Phys. 28 (1957).

15. Guinier, A.; Fournier, G.; Small Angle Scattering of X-rays; Wiley: New York, 1955.

16. Bonart, R.; Kolloid Z.Z. Polym. 194 (1964) 97.

17. Hosemann, R.; Polymer 3 (1962) 349.

Figure Captions

Fig. 1.   (a) Pole figures of (200) (020) (002) planes of oriented HDPE by rolling or by channeling-die compression. (b) Schematic diagram of crystallographic axes (a,b,c) and macroscopic specimen axes.

Fig. 2.   Electron micrographs of channel-die sample; (a) viewed parallel to the b-axis; (b) viewed parallel to the a-axis.

Fig. 3.   Electron micrographs of rolled sample; (a) viewed parallel to the b-axis; (b) viewed parallel to the a-axis.

Fig. 4.   2-D SAXS patterns of channel-die samples; (a) beam parallel to b-axis; (b) beam parallel; (c) 20°; (d) 40° to a-axis.

Fig. 5.   2-D SAXS patterns of rolled sample; (a) beam parallel to b-axis and at the center of cross section (b) at the edge of cross section; (c) beam parallel; (d) 20°; (e) 40° to a-axis.

Fig. 6.   (a) Schematic diagram of 2-D lamellar stacks sheared at different levels; (b) corresponding $A(q)$ and $Z(q)$ functions; (c) resulting 2-D small angle pattern obtained by superposing each pattern.

Fig. 7.   (a) Schematic diagram of 2-D lamellar stacks which are rotated by different amounts relative to the c-axis; (b) corresponding $A(q)$ and $Z(q)$ functions; (c) resulting 2-D SAXS pattern obtained by super-position.

Fig. 8.   Long-spacings of sheared lamellar stacks (D_θ) normalized by D of unsheared parallel stack.

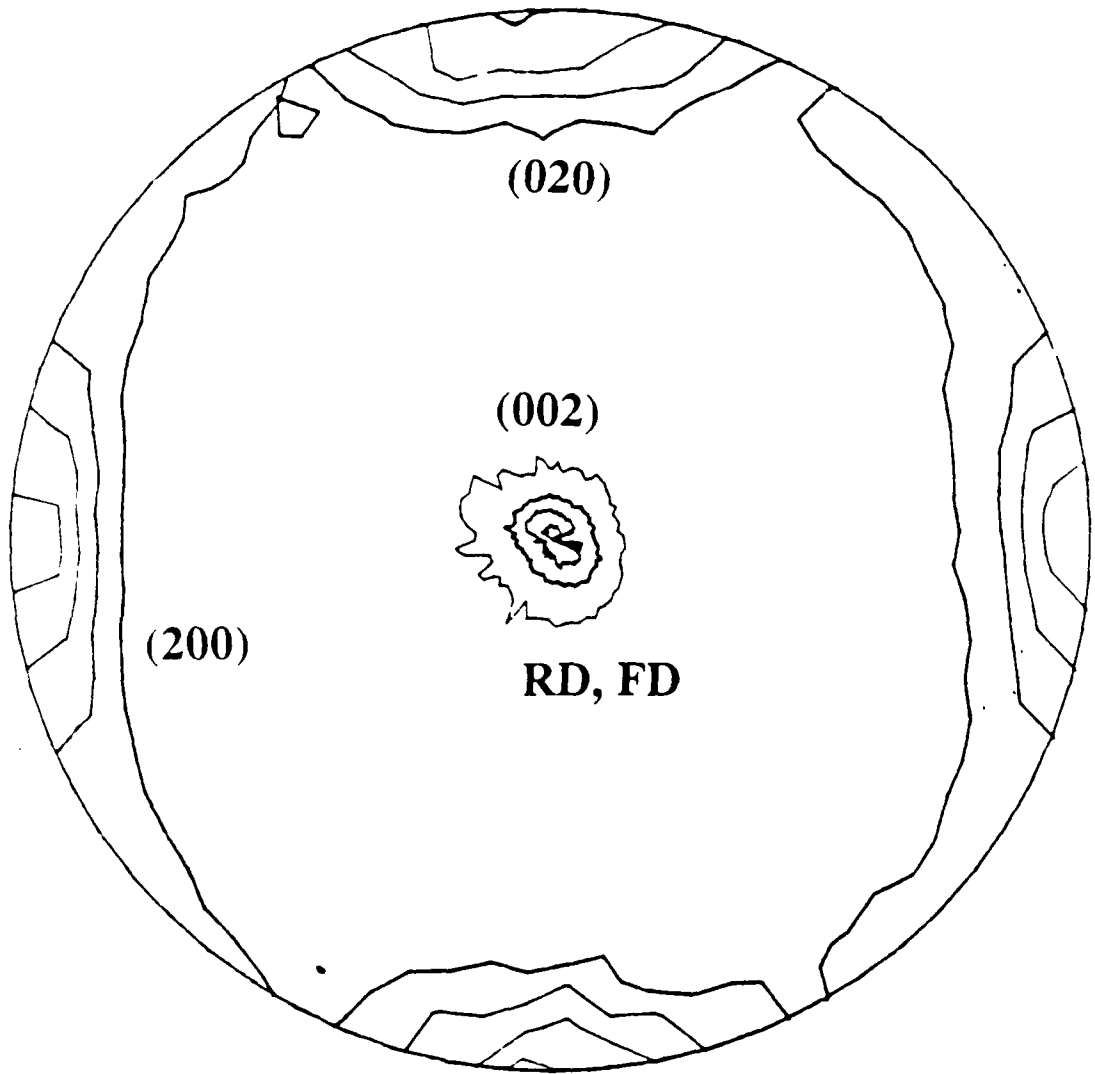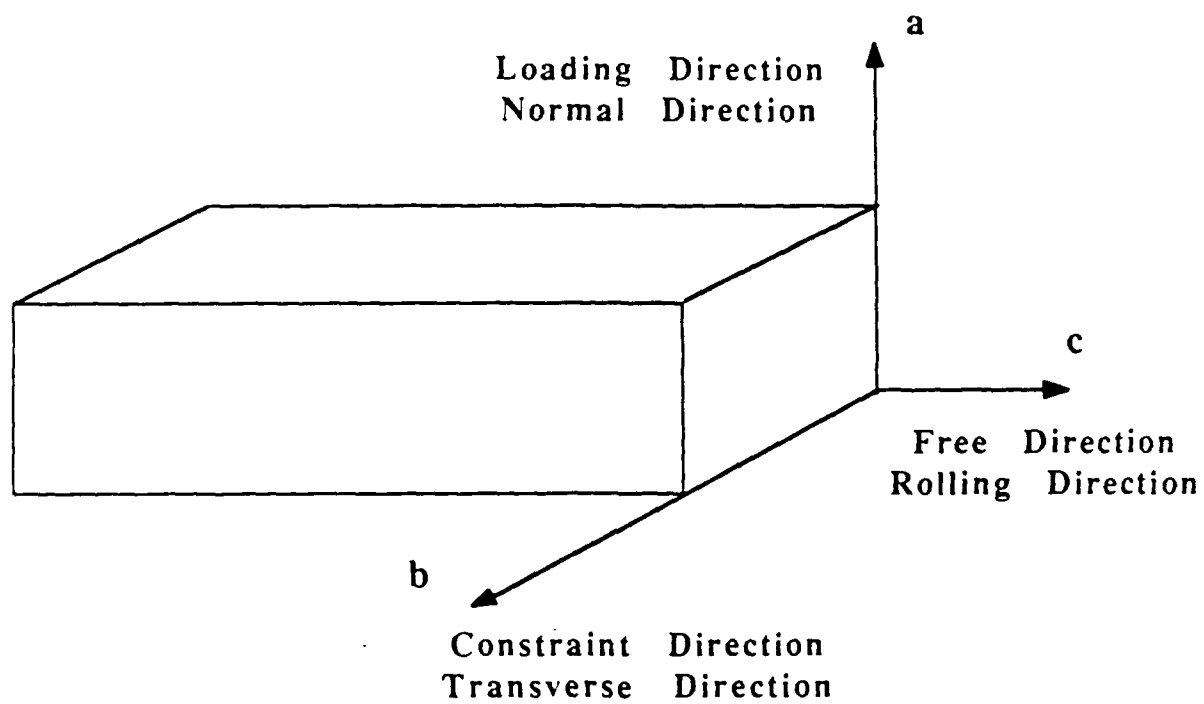Fig. 9.   Normalized SAXS intensity vs. tilt angle.

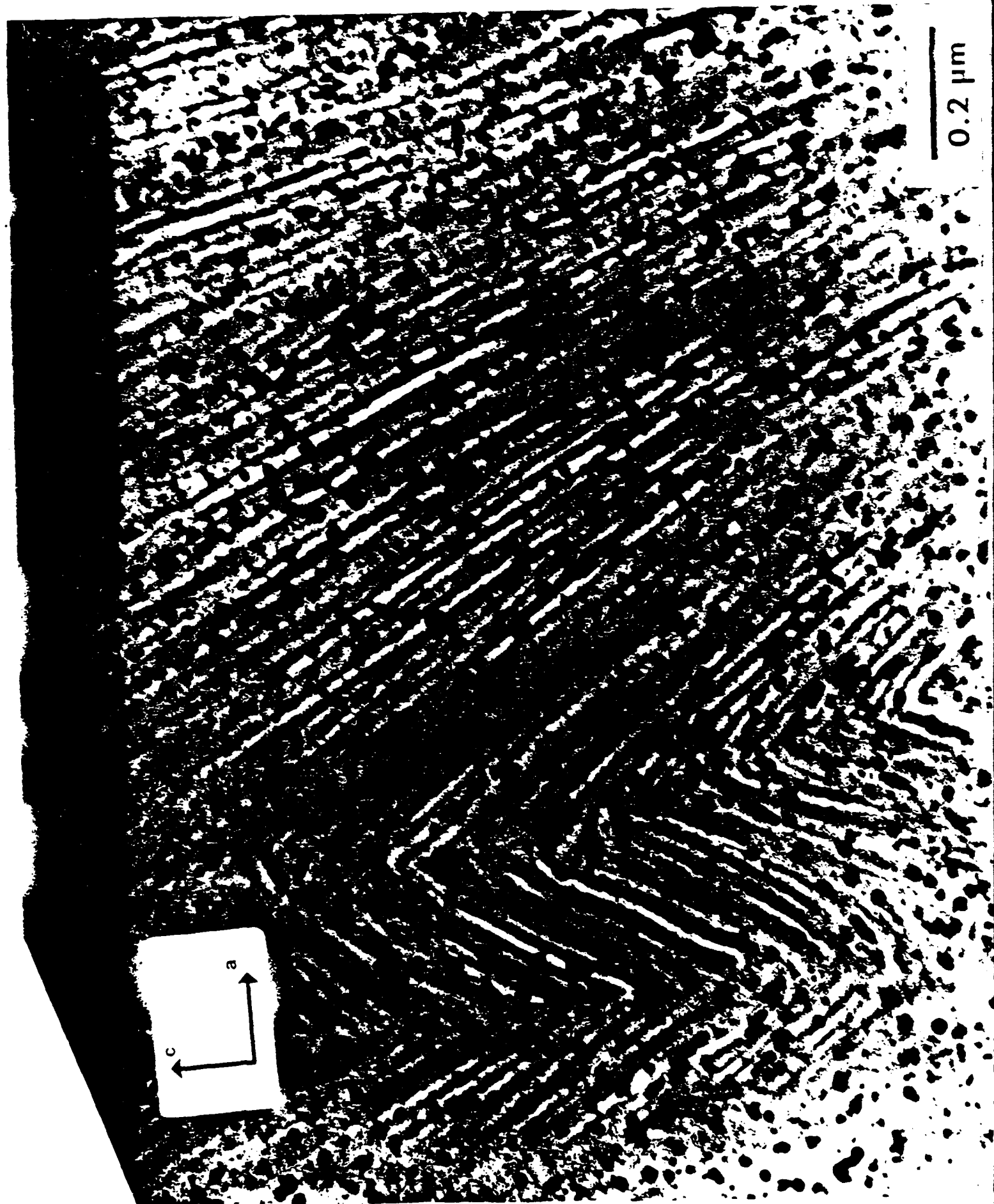Loading   Direction
Normal   Direction

a

c

Free   Direction
Rolling   Direction

b

Constraint   Direction
Transverse   Direction

(p)   (ɔ)   (q)

(ɐ)

(e)

(d)

(c)

(b)

(a)

(c)

(b)

(a)

$1/D$

D

$-\Theta_1$

$-\Theta_2$

A 2 (b)

Z 2(b)

q_1

q_3

Θ_1

Θ_2

$D\cos\Theta_1$

D

c

a

(c)

(b)

1/D

1/D

A$_2$(b)

Z(b)

b$_1$

Θ_2

b$_3$

1/D

(a)

D

a

c

Θ_2